**RESEARCH ARTICLE**

Determination of Hexachlorocyclohexane by Gas Chromatography Combined with Femtosecond Laser Ionization Mass Spectrometry

Xixiang Yang,[1] Tomoko Imasaka,[2] Adan Li,[3,4] Totaro Imasaka[3]

[1]Department of Applied Chemistry, Graduate School of Engineering, Kyushu University, 744 Motooka, Nishi-ku, Fukuoka 819-0395, Japan
[2]Laboratory of Chemistry, Graduate School of Design, Kyushu University, 4-9-1 Shiobaru, Minami-ku, Fukuoka 815-8540, Japan
[3]Division of International Strategy, Center of Future Chemistry, Kyushu University, 744 Motooka, Nishi-ku, Fukuoka 819-0395, Japan
[4]College of Environmental and Chemical Engineering, Yanshan University, Qinhuangdao, 066004, China
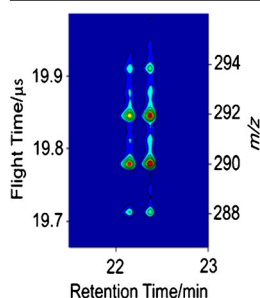
Abstract. Structural isomers and enantiomers of hexachlorocyclohexane (HCH) were separated using a chiral column by gas chromatography and quantitatively determined by multiphoton ionization mass spectrometry using an ultraviolet femtosecond laser (200 and 267 nm) as the ionization source. The order of elution of the enantiomers (i.e., (+)-α-HCH and (-)-α-HCH) was predicted from stabilization energies calculated for the complexes using permethylated γ-cyclodextrin as the stationary phase of the column, and the results were compared with the experimental data. The molecular ions observed for HCH were weak, even though they can be ionized through a process of resonance enhanced two-photon ionization at 200 nm. This unfavorable result can be attributed to the dissociation of the molecular ion, as predicted from quantum chemical calculations.

Keywords: Gas chromatography, Mass spectrometry, Laser ionization, Hexachlorocyclohexane, Pesticide

Introduction

During the past several decades, varieties of pesticides have been developed and are currently in widespread use for pest control to increase the yields of agricultural crops. Most are toxic and are harmful, not only for insects but also for humans [1–3]. Because of this, the use of pesticides should be carefully controlled, in order to protect the environment. Hexachlorocyclohexane (HCH), a compound that was previously used as a component of some types of pesticides, is the most abundant organochlorine compound remaining in the atmosphere and is also found in water [4–8]. Although the use of HCH was prohibited a long time ago, it still can be found in the environment because of its high chemical stability. It should be noted that HCH derivatives are still used in several countries when their use is more beneficial than the detriment resulting from the contamination of the environment. HCH is a generic term for isomers of 1,2,3,4,5,6,-hexachlorocyclohexane, and these isomers are denoted by Greek letters (i.e., α-, β-, γ-, δ-, ε-, η-, and θ-HCH) [9]. Commercial products are composed of a mixture of the above isomers, and typically contain 60%–70% of α-, 5%–12% of β-, 10%–15% of γ-HCH [10]. The order of toxicity for insects is reported to be γ > α > δ >> β [11]. These HCHs primarily affect the central nervous system (CNS). Although the mechanism responsible for its toxicity in the human body remains mostly unknown, the α-, γ-, and δ-HCH isomers are considered to be CNS depressants [12]. Only α-HCH consists of chiral isomers [13]. The enantiomeric ratio of (+)-α-HCH and (-)-α-HCH in water from the North Sea has been measured [14]. The ratio for technical α-HCH is reported to be 0.99 ± 0.02, but the value changes from 1.2 to 1.9 in the case of blubber, liver, and lungs of neonatal northern fur seals [15]. Although α-, β-, and γ-HCHs were recently issued as new persistent organic pollutants (POPs) by the

Correspondence to: Totaro Imasaka; e-mail: imasaka@cstf.kyushu–u.ac.jp

Stockholm Convention, toxic, persistent, and bio-accumulative HCHs, mainly consisting of α-HCH (80%) and β-HCH, remain in the environment and are estimated to be 4–7 million tons [16].

The distribution of the structural and enantiomeric isomers provides important information for assessing the environment and also for identifying sources of HCH production. However, the levels of the toxic pesticides are low, and numerous species that interfere with their analysis are present at high concentrations [17]. Therefore, developing a sensitive as well as a selective analytical method for the analysis of such compounds would be highly desirable. To date, several types of analytical instruments have been employed to achieve this goal, e.g., gas chromatography/mass spectrometry (GC/MS) [18, 19], liquid chromatography/mass spectrometry (LC/MS) [20–22], and liquid chromatography/tandem mass spectrometry (LC/MS-MS) [21]. In standard GC/MS, electron ionization (EI) has been used successfully, since standard MS data are available for many organic compounds in databases and the analyte can be readily assigned. However, other ionization techniques such as photoionization are also useful for trace analysis. For example, femtogram detection limits for dioxins and subfemtogram detection limits for polycyclic aromatic hydrocarbons have been reported [23]. Several pesticides have absorption bands at around 200 nm, and a far-ultraviolet femtosecond laser (200 nm) has been advantageously used for more efficient ionization in MS [24].

In this study, we report on the separation of four structural isomers of α-, β-, γ-, δ-HCHs and two enantiomers of α-HCH [i.e., (+)-α-HCH and (−)-α-HCH] using a capillary column with a stationary phase consisting of permethylated γ-cyclodextrin (PM-γ-CD) and their determination by MS using a femtosecond laser emitting in the deep-ultraviolet (267 nm) and far-ultraviolet (200 nm) regions. The order of elution of the (±)-α-HCH enantiomers were theoretically predicted from the data obtained by stabilization energy calculations by a technique based on molecular dynamics using a semi-empirical method. The mechanism of fragmentation is discussed using data obtained by quantum chemical calculations.

Experimental

Apparatus

The analytical instrument used in this study was reported in detail elsewhere [25, 26]. Briefly, a 1-μL volume of sample solution was injected into a GC (6890N; Agilent Technologies, Santa Clara, CA, USA) that was combined with a time-of-flight mass spectrometer (TOFMS) developed in our laboratory; this instrument is now commercially available (HGK-1; Hikari-GK, Fukuoka, Japan). The third and fourth harmonic emissions (267 and 200 nm) of a Ti:sapphire laser (800 nm, 35 fs, 1 kHz, 4 mJ, Elite; Coherent Inc., CA, USA) were used as the ionization source. The laser beam was focused on a molecular beam for multiphoton ionization (MPI). The analytes in a standard sample mixture containing four structural isomers of HCHs were separated using a capillary column with a chiral stationary phase (PM-γ-CD, γ-DEX 120 column, 30 m long, 0.25 mm inner diameter, 0.25 mm film thickness; Supelco, Bellefonte, PA, USA). The temperature of the GC oven was programmed to increase from 100 °C (1 min hold) to 150 °C at a rate of 20 °C/min and then to 190 °C at a rate of 2 °C, after which it was held for 15 min. The temperature was further increased to 210 °C at a rate of 30 °C and was then held for 5 min. The flow rate of helium used as a carrier gas was 1 mL/min. The ions induced in the MS were accelerated toward a TOF tube and were detected by microchannel plates (F4655-11; Hamamatsu Photonics, Shizuoka, Japan). The mass spectrometer was optimized by continuously introducing pentachlorobenzene, and the mass resolution achieved was 750 and 800 when measured at 267 and 200 nm, respectively. The signals were recorded by a digitizer (AP240, Acqiris; Agilent Technologies), and the data were analyzed using home-made software programmed by LabVIEW.

Reagents

Enantiomeric isomers of (±)-α-HCH and δ-HCH were purchased from Wako Pure Chemical Industries, Tokyo, Japan. β-HCH was supplied by Sigma Aldrich Japan, Tokyo, Japan, while γ-HCH was a product of Tokyo Chemical Industry, Tokyo, Japan. Acetone (analytical grade), used as a solvent, was supplied from Wako Pure Chemical Industries.

Quantum Chemical Calculation

To investigate the mechanism for the ionization, the spectral properties such as the ionization energies and the absorption spectra of α-, β-, γ-, and δ-HCH in the gaseous phase are necessary. For this purpose, sophisticated analytical instruments are required for photoelectron spectroscopy and also for absorption spectrometry in the vacuum-ultraviolet region. Then, these parameters were evaluated using data obtained by quantum chemical calculations in this study. The optimized geometry of the ground state and the harmonic frequencies were calculated using the B3LYP method based on density functional theory (DFT) with a cc-pVDZ basis set. The lowest 40 singlet transition energies and the oscillator strengths were calculated using time-dependent DFT (TD-DFT), and the absorption spectra were predicted by assuming a peak with a Gaussian profile having a half width at half maximum of 0.333 eV. These calculations were performed using the Gaussian 09 and Gauss View 5 programs [27, 28]. For the discussion of fragmentation, the enthalpy change by the dissociation of a molecular ion was calculated using DFT.

In order to examine the energy of interaction between (±)-α-HCH and PM-γ-CD, their structures were generated using Gauss View 5.0.9 and were optimized at the level of PM3 (Parameterized Model number 3) using Gaussian 09. As an initial configuration of PM-γ-CD, the glycosidic oxygen atoms (i.e., Oa, Ob, Oc, and Od) were placed on the XY plane and their center of gravity was positioned at the origin of the space-fixed Cartesian coordinate of XYZ (see Figure 1 for details).
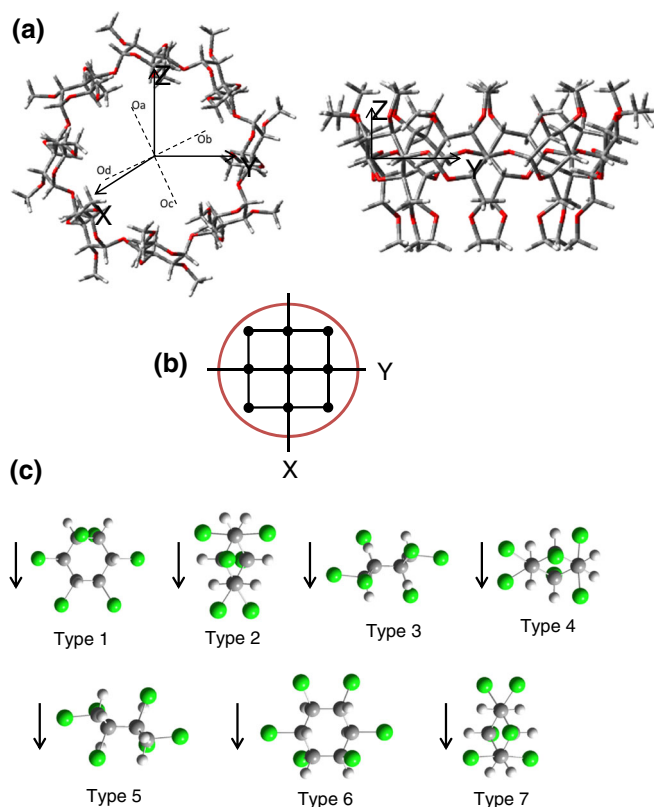
Figure 1. (**a**) Structure of PM-γ-CD calculated at the PM3 levels. Red, oxygen; gray, carbon; white, hydrogen. (**b**) Cartesian coordinate viewed from a ring with a larger size at a height of Z = 5 Å. The locations initially used for the simulation are indicated as black filled circles in the image. The spacing between the locations is 1.5 Å. (**c**) Initial configuration of (+)-α-HCH isomers used in the simulation. Type 1, original position (not rotated); Type 2, rotated 90° around the z-axis; Types 3–5, rotated 90° around the y-axis and rotated 0°, 90°, 180° around the z-axis, respectively; Types 6–7, rotated 180° around the y-axis and rotated 0°, 90° around the z-axis, respectively. A configuration obtained by rotating 180° around the z-axis and a configuration obtained by rotating 180° around the y-axis and the z-axis were equivalent to Type 1 and Type 6, respectively, and they were not used in the computation. The arrow shows the direction that (+)-α-HCH approaches PM-γ-CD. Green, chlorine; dark gray, carbon; light gray, hydrogen

The methylated secondary hydroxyl groups of the PM-γ-CD (i.e., –OCH$_3$ were set to point toward the positive direction of the Z-axis. The (±)-α-HCH molecule was assumed to approach toward the wide rim of the PM-γ-CD.

Results and Discussion

Spectral Properties of HCHs

Absorption spectra of HCH isomers calculated by DFT are shown in Figure 2. The energy of excitation to the first singlet electronic excited state (*EE*) is located at around 200 nm while no absorption band is found at around 267 nm. Half of the energy for ionization (*IE*/2) is located at around 250 nm,

suggesting two-photon ionization at 200 nm and three-photon ionization at 267 nm. Thus, all of the isomers would be ionized through a resonant two-photon ionization at 200 nm and non-resonant three-photon ionization at 267 nm. Therefore, a far-ultraviolet laser (200 nm) would be preferential for efficient ionization and also for reducing the excess energy to suppress fragmentation. The molar absorptivity at 200 nm was ca. 500, 700, 400, and 400 for α-, β-, γ-, and δ-HCHs, respectively, which was nearly identical to each other. This suggests that the ionization efficiency would not change significantly among these isomers.

Predicted Elution Order of (±)-α-HCHs

The optimized structure of the PM-γ-CD used as the stationary phase of the capillary column in GC is shown in Figure 1a, and suggests that the molecule has a symmetry of C$_8$. The average distance from the center of gravity to a glycosidic oxygen atom, Oa, Ob, Oc, Od, of PM-γ-CD was 5.94 Å, which was similar to the value of 5.88 Å reported based on X-ray crystallography data for γ-CD [29]. The average angle of C-O-C calculated for a glycosidic oxygen was 115°, which was close to the observed value of 117°. The average distance between the oxygen atoms was 4.54 Å, which is nearly identical to the observed value (4.50 Å). Thus, the calculated structural data are in reasonably good agreement with the observed data for γ-CD, although no data were available for PM-γ-CD as a reference. It should also be noted that the calculated structure of PM-γ-CD was very similar to that obtained by increasing the number of the glycosidic units from seven to eight in the reported structure of PM-β-CD [30].

Since the (±)-α-HCH/PM-γ-CD complex consists of 258 atoms, finding an optimized structure required a long time or it was difficult to converge the data in the DFT computation: it was difficult to apply even the Hartree-Fock method. Therefore, a semi-empirical method (i.e., PM3) was utilized in this study. A preliminary examination suggests that the calculated value for the stabilization energy by complexing was affected by the initial position and configuration of (±)-α-HCH. In fact, (±)-α-HCH with different configurations placed at various locations approaches the PM-γ-CD cage in the experiment, and enantiomeric separation was achieved by virtue of the small difference in the stabilization energy of the complex of (±)-α-HCH and PM-γ-CD. The (±)-α-HCHs with different configurations were then positioned at 3 × 3 grids above the PM-γ-CD before the calculation (see Figure 1b). A molecule was assumed to approach along the Z-axis toward the inner surface of the PM-γ-CD cage. To investigate the stabilization energy along the Z-axis, the structure of the (±)-α-HCH/PM-γ-CD complex was first optimized with no restrictions by placing the center of gravity of (±)-α-HCH at (0, 0, Z) where Z = 3, 4, 5, 6, 7 Å. The energy was minimal at (0, 0, 5 Å) in the cases of both (+)-α-HCH and (−)-α-HCH. Second, the initial center of gravity was set at (X, Y, Z = 5 Å) where X = −1.5, 0, 1.5 and Y = −1.5, 0, 1.5,
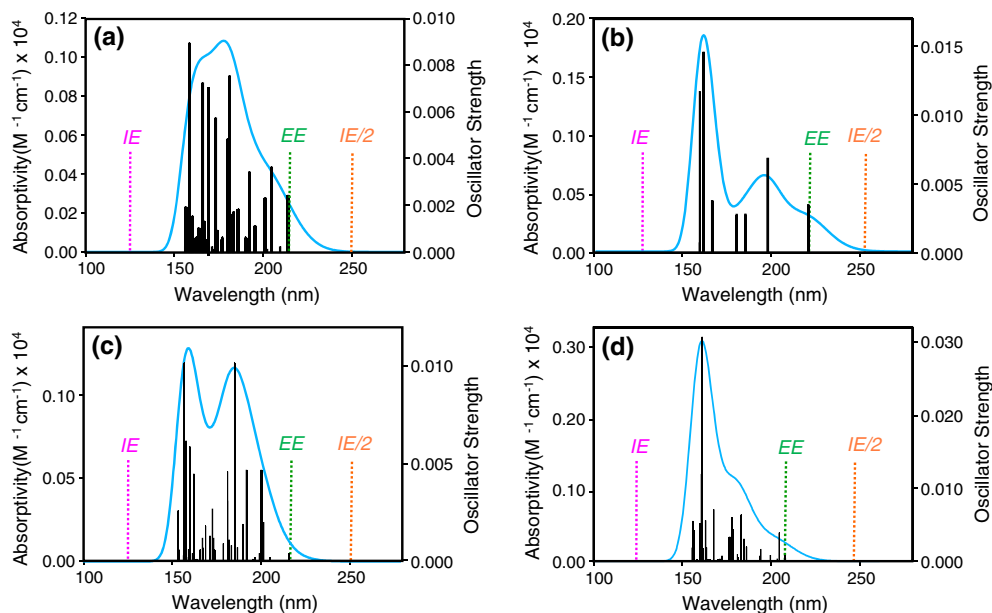
Figure 2. Absorption spectra calculated for (**a**) α-HCH, (**b**) β-HCH, (**c**) γ-HCH, (**d**) δ-HCH by DFT. *IE*, ionization energy; *IE*/2, half of ionization energy; *EE*, excitation energy to the first electronic excited state. The vertical ionization energy for these compounds are 9.91 eV (125.1 nm), 9.91 eV (125.1 nm), 9.87 eV (125.6 nm), and 10.08 eV (123.0 nm), respectively

since (±)-α-HCH is assumed to approach from various positions toward the wider rim of the PM-γ-CD. The (±)-α-HCH molecule was then rotated by 0°, 90°, 180° around the z-axis of the molecule-fixed Cartesian coordinate of xyz and was also rotated by 0°, 90°, 180° around the y-axis, as shown Figure 1c; the arrow in the figure shows the direction of approach to the PM-γ-CD. The optimization was then initiated from 126 positions/configurations/species (i.e., 9 translational × 7 rotational × 2 (±)-α-HCH species. After rejecting data leading to unstable and deformed structures (12/126), the difference in the stabilization energies for the (±)-α-HCHs was calculated to be −0.34 ± 1.42 kcal/mol, suggesting that the (+)-α-HCH/PM-γ-CD complex is slightly more stable than the (−)-α-HCH/PM-γ-CD complex: the conclusion remained unchanged even when the conditions for the calculation and the rule for rejecting the data were modified. A small difference in the stabilization energy could be due to the very flexible structure of PM-γ-CD. Thus, (+)-α-HCH would be predicted to elute later than (−)-α-HCH in GC, as reported in the literature [31].

Determination of HCHs

A sample containing a mixture of α-, β-, γ-, and δ-HCH was analyzed by GC/MPI-TOFMS using a femtosecond laser emitting at 200 nm and the result is shown in Figure 3. The isomers of HCH were clearly separated by GC and a series of fragment peaks were produced in MS. The expanded view shown in the insert indicates the complete separation/resolution of (+)-α-HCH and (−)-α-HCH by GC and MS; the (−)-enantiomer elutes earlier than the (+)-enantiomer in GC [31]. The signal intensity of the peak arising from β-HCH is relatively weak, although the

molar absorptivity is slightly higher than that for the other compounds at 200 nm, suggesting that a β-HCH undergoes a more inefficient ionization from the excited state. A two-dimensional display measured at 267 nm is shown in Figure 4 for comparison. A molecular ion is more clearly observed for α- and γ-HCHs at 200 nm than at 267 nm, which would be attributed to efficient resonant two-photon ionization at 200 nm and inefficient non-resonant three-photon ionization at 257 nm. However, no drastic changes were observed for data measured
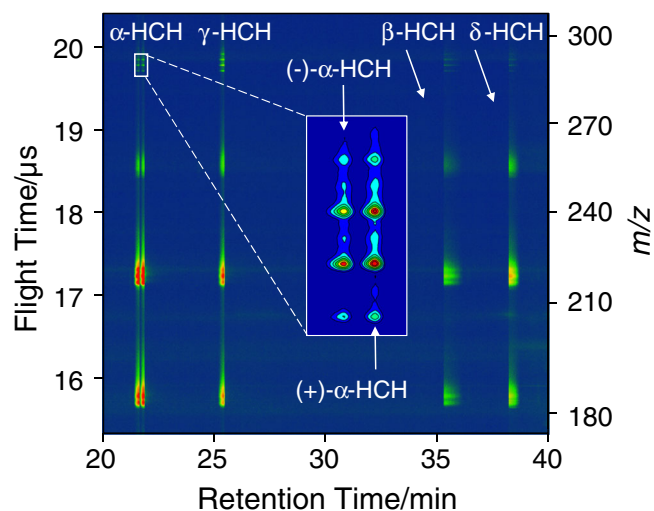

Figure 3. Two-dimensional display for a sample mixture containing four isomers of α-, β-, γ-, and δ-HCHs measured at 200 nm (20 µJ). The insert shows the expanded view where the molecular ions of (±)-α-HCH enantiomers appear. A series of isotopomers consisting of $^{35}Cl/^{37}Cl$ and $^{12}C/^{13}C$ are observed in the expanded view. The concentration of the analyte was 25 ng/µL for each isomer of HCH

at the different wavelengths, suggesting that the effect of reso-
nance is minimal in femtosecond ionization [32].

Fragmentation of HCHs

As shown in Figures 3 and 4, the fragment patterns are similar
among these isomers, although α- and γ-HCHs give rise to a
more pronounced molecular ion and the signal intensity is
larger when measured at 200 nm. Figure 5 shows the mass
spectra of HCHs extracted from the data shown in Figure 3. A
molecular ion corresponding to $C_6H_6{}^{35}Cl_6$ is clearly observed
at m/z = 288, in addition to other several isotopomers of
$C_6H_6{}^{35}Cl_{6-x}{}^{37}Cl_x$ where x = 1–3. The EI mass spectra are
available for HCHs in the NIST database: the spectral region
of a molecule ion is missing for α-HCH, probably due to a
small signal intensity (http://webbook.nist.gov/cgi/cbook.cgi?
ID=C319846&Units=SI&Mask=200#Mass-Spec, http://
webbook.nist.gov/cgi/cbook.cgi?ID=C319857&Units=
SI&Mask=200#Mass-Spec, http://webbook.nist.gov/cgi/
cbook.cgi?ID=C58899&Units=SI&Mask=200#Mass-Spec,
http://webbook.nist.gov/cgi/cbook.cgi?ID=C319868&Units=
SI&Mask=200#Mass-Spec). The relative signal intensities of
the molecular ions were apparently more enhanced in the MPI
mass spectra measured at 200 nm. This result suggests that UV
femtosecond ionization is more favorable for observing a
molecular ion. It should be noted that the signal of the
fragment, $[M-HCl]^+$ observed at around m/z = 253 in
Figure 5, is very broad, which is in contrast to the result for
$[M-HCl_2]^+$ providing a slightly split structure. In this study, a
linear-type TOFMS was used and the initial velocity distribu-
tion of the ion can be evaluated; the mass resolution calculated
using the signal of a molecular ion was $m/\Delta m$ = 520 and this
peak broadening cannot be attributed to the limited resolution
of the mass spectrometer. These results suggest that a molecule
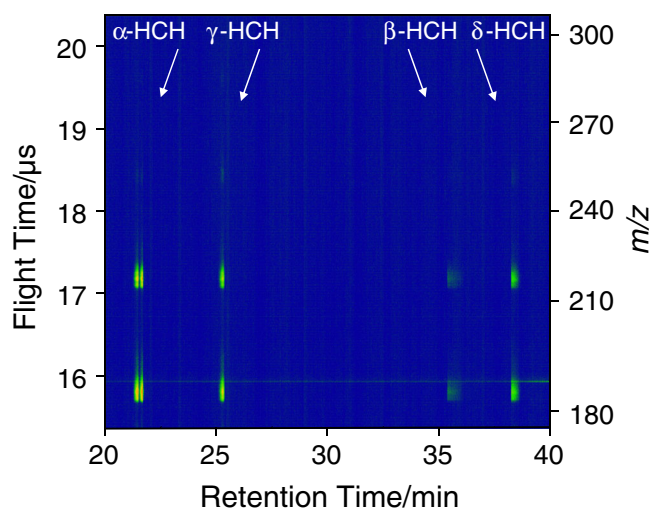easily dissociates to form fragment ions and neutral species

Figure 5. Mass spectra of HCHs measured at 200 nm (20 μJ)

Figure 4. Two-dimensional display for a sample mixture con-
taining four isomers and α-, β-, γ-, δ-HCHs measured at 267 nm
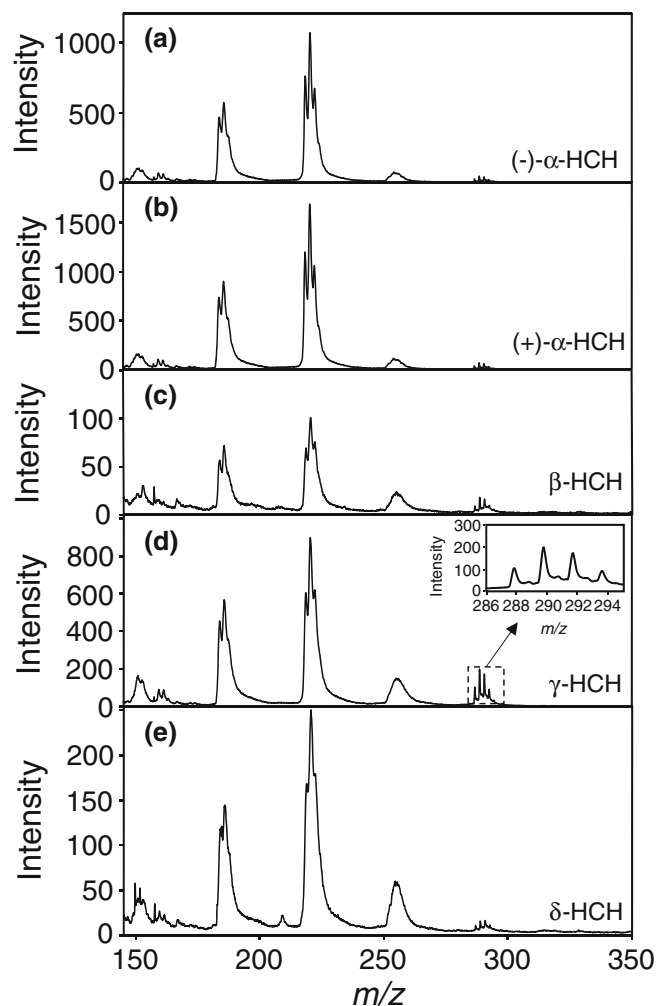(20 μJ). The concentration of the analyte was 25 ng/μL for each
isomer of HCH

such as HCl (process A) or HCl_2 (process B): these processes
would occur in parallel (not sequentially) in femtosecond ion-
ization mass spectrometry. The dissociation releases the excess
energy as translational energies of the ions and also of the
neutral species. Concerning the fragmentation, an enthalpy
change in processes A and B was calculated by DFT. In process
A, the enthalpy change was –8.2, –12.0, –3.3, and –5.8 kcal/
mol for α-, β-, γ-, and δ-HCH, respectively, suggesting that the
molecular ion can be stabilized by producing a fragment ion
and a neutral species of HCl and that the fragmentation is less
efficient for γ-HCH. Accordingly, a very broad peak was
observed for the fragment of $[M-HCl]^+$ and a molecular ion
remained more efficiently for γ-HCH due to a smaller change
in enthalpy (–3.3 kcal/mol or –0.14 eV). In process B, the
enthalpy change was 7.8, 0.0, 8.4, 6.2 kcal/mol for α-, β-, γ-,
and δ-HCH, respectively. Then, a small energy is required for
the dissociation of HCl_2 (e.g., 8.4 kcal/mol or 0.37 eV for γ-
HCH), which is, however, much smaller than the excess energy
in two-photon ionization (6.20 × 2 – 9.87 = 2.53 eV): a
molecular ion remained more efficiently for γ-HCH due to a
larger change in enthalpy. Thus, a slightly split structure was
observed for the fragment of $[M-HCl_2]^+$ and a molecular ion

remained more efficiently for γ-HCH. When the third harmonic emission (267 nm) was used, the excess energy obtained through the process of three-photon ionization increases significantly ($4.64 \times 3 - 9.87 = 4.05$ eV), suggesting that a molecular ion can more easily dissociate to form fragment ions. It is interesting to note that a molecular ion was observed more efficiently at 800 nm rather than at 400 nm for benzene and halogenated ethylenes (both through non-resonant MPI processes) [33, 34]. Then, a fundamental beam of the Ti:sapphire laser was utilized in this study to examine the advantage of this technique for observing a molecular ion. However, it was difficult to observe a molecular ion at 800 nm under the optimized conditions used in this study. In fact, the fundamental beam (800 nm) was employed for dissociation of the protonated peptides formed by electrospray ionization (ESI) [35]. Thus, moderate resonant two-photon ionization in the ultraviolet region would be more preferential, although further studies would be necessary to conclude this discussion. It has been reported that the efficiency of non-resonant two-photon ionization can be improved significantly by optimizing the wavelength and decreasing the pulse width of the femtosecond laser (<100 fs) [32]. Therefore, a tunable ultraviolet femtosecond laser, the wavelength of which can be optimized to reduce excess energy at around 250 nm, would be useful to understand the mechanism for non-resonant or nearly-resonant two-photon ionization in terms of observing a molecular ion [36].

Limit of Detection

Figure 6 shows a two-dimensional display obtained using the third harmonic emission (267 nm) at a larger pulse energy available (75 µJ). Because the signal intensity was increased and a molecular ion was observed for γ-HCH, an analytical curve was constructed and confirmed to be linear in a range of 0–12 ng/µL under present conditions. The limit of detection (LOD) was 68 pg/µL when the signal intensity was measured
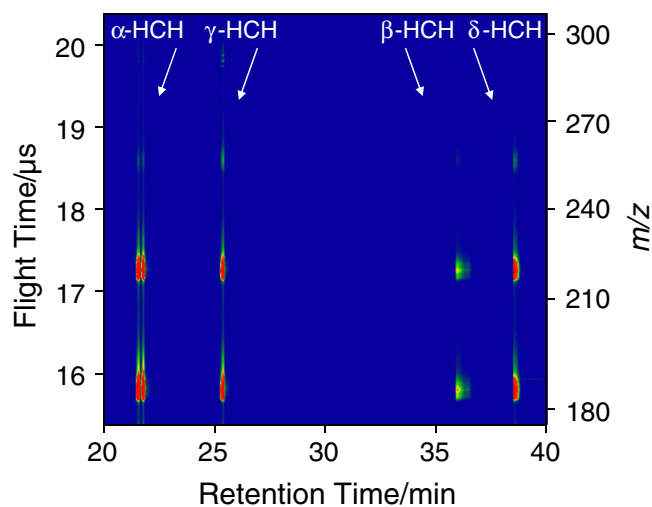
for a molecular ion ($m/z = 290$). The value was improved to 5.0 pg/µL when a fragment ion ($m/z = 219$) was measured. The rather poor detection limits compared with those reported for other organic compounds such as polycyclic aromatic hydrocarbons [23] can be attributed to inefficient non-resonant three-photon ionization and the efficient dissociation of a molecular ion to fragments.

Conclusions

In this study, we report on the separation of some isomers and enantiomers of HCHs using a capillary column with a chiral stationary phase (PM-γ-CD) by GC. A molecular ion was more clearly observed for the isomers of α- and γ-HCHs but was weak, even when a far-ultraviolet femtosecond laser (200 nm) was used for resonant two-photon ionization. This result can be explained by the efficient dissociation of neutral species such as HCl and HCl_2 from the molecular ion using data obtained by quantum chemical calculations. The isomers and enantiomers of the HCHs were separated by GC and their isotopomers were identified by MS on the two-dimensional display data, suggesting the potential advantage of this method for the comprehensive analysis of pesticides in the environment.

Acknowledgments

Figure 6. Two-dimensional display for a sample mixture containing four isomers of α-, β-, γ-, and δ-HCHs measured at 267 nm (75 µJ). The concentration of the analyte was 10 ng/µL for each isomer of HCH

References

1. Bucheli, T.D., Grüebler, F.C., Müller, S.R., Schwarzenbach, R.P.: Simultaneous determination of neutral and acidic pesticides in natural waters at the low nanogram per liter level. Anal. Chem. **69**, 1569–1576 (1997)

2. Tsai, W.C., Huang, S.D.: Dispersive liquid–liquid microextraction with little solvent consumption combined with gas chromatography-mass spectrometry for the pretreatment of organochlorine pesticides in aqueous samples. J. Chromatogr. A **1261**, 5171–5175 (2009)

3. Li, J., Zhang, G., Qi, S., Li, X., Peng, X.: Concentrations, enantiomeric compositions, and sources of HCH, DDT and chlordane in soils from the Pearl River Delta South China. Sci. Total Environ. **372**, 215–224 (2006)

4. Iwata, H., Tanabe, S., Ueda, K., Tatsukawa, R.: Persistent organochlorine residues in air, water, sediments, and soils from the Lake Baikal Region Russia. Environ. Sci. Technol. **29**, 792–801 (1995)

5. Walker, K.: Factors influencing the distribution of lindane and other hexachlorocyclohexanes in the environment. Environ. Sci. Technol. **33**, 4373–4378 (1999)

6. Simonich, S.L., Hites, R.A.: Global distribution of persistent organochlorine compounds. Science **269**, 1851–1854 (1995)

7. Montgomery, J.H.: Agrochemical Desk Reference, Environmental Data, Chelsea, MI, 248–251 (1993).

8. Li, Y., Bidleman, T., Barrie, L., McConnell, L.: Global hexachlorocyclohexane use trends and their impact on the arctic atmospheric environment. Geophys. Res. Lett. **25**, 39–41 (1998)

9. Wilett, K., Ulrich, E., Hites, R.: Differential toxicity and environmental fates of hexachlorocyclohexane isomers. Environ. Sci. Technol. **32**, 2197–2207 (1998)

10. Kutz, F.W., Wood, P.H., Bottimore, D.P.: Organochlorine pesticides and polychlorinated biphenyls in human adipose tissue. Rev. Environ. Contam. Toxicol. **120**, 1–82 (1991)
11. Marrs, T.T., Ballantyne, B.: Pesticide Toxicology and International Regulation. John Wiley and Sons, Ltd., 34. Hobuken, New Jersey (2004)
12. Pomes, A., Rodriguez-Farre, E., Sunol, C.: Inhibition of t-[^{35}S]butylbicyclophosphorothionate binding by convulsant agents in primary cultures of cerebellar neurons. Dev. Brain Res. **73**, 85–90 (1993)
13. Cristol, S.: The structure of α-benzene hexachloride. J. Am. Chem. Soc. **71**, 1894 (1949)
14. Faller, J., Huhnerfuss, H., Konig, W., Krebber, R., Ludwig, P.: Do marine bacteria degrade o-hexachlorocyclohexane stereoselectively? Environ. Sci. Technol. **25**, 676–678 (1991)
15. Mössner, S., Spraker, T., Becker, P., Ballschmiter, K.: Ratios of enantiomers of alpha-HCH and determination of alpha-, beta-, and gamma-HCH isomers in brain and other tissues of neonatal Northern fur seals (*Callorhinus ursinus*). Chemosphere **24**, 1171–1180 (1992)
16. Vijgen, J., Abhilash, P., Li, Y., Lal, F., Forter, M., Torres, J., Singh, N., Yunus, M., Tian, C., Schäffer, A., Weber, R.: Hexachlorocyclohexane (HCH) as new Stockholm Convention POPs—a global perspective on the management of Lindane and its waste isomers. Environ. Sci. Pollut. Res. **18**, 152–162 (2011)
17. Pinto, M., Sontag, G., Bernardino, R., Noronha, J.: Pesticides in water and the performance of the liquid-phase microextraction based techniques. A review. Microchem. J. **96**, 225–237 (2010)
18. Berger, M., Loffler, D., Ternes, T., Heiniger, P., Ricking, M.: Hexachlorocyclohexane derivatives in industrial waste and samples from a contaminated riverine system. Chemosphere **150**, 219–226 (2016)
19. Barrek, S., Cren-Olivé, C., Wiest, L., Baudot, R., Arnaudguilhem, C., Grenier-Loustalot, M.: Multi-residue analysis and ultra-trace quantification of 36 priority substances from the European Water Framework Directive by GC-MS and LC-FLD-MS/MS in surface waters. Talanta **79**, 712–722 (2009)
20. Xu, W., Wang, X., Cai, Z.: Analytical chemistry of the persistent organic pollutants identified in the Stockholm Convention: a review. Anal. Chim. Acta **790**, 1–13 (2013)
21. Trtić-Petrović, T., Đorđević, J., Dujaković, N., Kumrić, K., Vasiljević, T., Laušević, M.: Determination of selected pesticides in environmental water by employing liquid-phase microextraction and liquid chromatography-tandem mass spectrometry. Anal. Bioanal. Chem. **397**, 2233–2243 (2010)
22. Bossi, R., Vejrup, K.V., Mogensen, B.B., Asman, W.A.H.: Analysis of polar pesticides in rainwater in Denmark by liquid chromatography-tandem mass spectrometry. J. Chromatogr. A **957**, 27–36 (2002)
23. Matsui, T., Fukazawa, K., Fujimoto, M., Imasaka, T.: Analysis of persistent organic pollutants at sub-femtogram levels using a high-power picosecond laser for multiphoton ionization in conjunction with gas chromatography/time-of-flight mass spectrometry. Anal. Sci. **28**, 445–450 (2012)
24. Hashiguchi, Y., Zaitsu, S., Imasaka, T.: Ionization of pesticides using a far-ultraviolet femtosecond laser in gas chromatography/time-of-flight mass spectrometry. Anal. Bioanal. Chem. **405**, 7053–7059 (2013)
25. Matsumoto, J., Saito, G., Imasaka, T.: Use of ring-repeller, double-skimmer electrodes for efficient ion focusing in mass spectrometry. Anal. Sci. **18**, 567–570 (2002)
26. Matsumoto, J., Nakano, B., Imasaka, T.: Development of a compact supersonic jet/multiphoton ionization/time-of-flight mass spectrometer for the on-site analysis of dioxin Part I: Evaluation of basic performance. Anal. Sci. **19**, 379–382 (2003)
27. Frisch, M.J., Trucks, G.W., Schlegel, H.B., Scuseria, G.E., Robb, M.A., Cheeseman, J.R., Scalmani, G., Barone, V., Mennucci, B., Petersson, G.A., Nakatsuji, H., Caricato, M., Li, X., Hratchian, H.P., Izmaylov, A.F., Bloino, J., Zheng, G., Sonnenberg, J.L., Hada, M., Ehara, M., Toyota, K., Fukuda, R., Hasegawa, J., Ishida, M., Nakajima, T., Honda, Y., Kitao, O., Nakai, H., Vreven, T., Montgomery, J.A., Jr., Peralta, J.E., Ogliaro, F., Bearpark, M., Heyd, J.J., Brothers, E., Kudin, K.N., Staroverov, V.N., Kobayashi, R., Normand, J., Raghavachari, K., Rendell, A., Burant, J.C., Iyengar, S.S., Tomasi, J., Cossi, M., Rega, N., Millam, J.M., Klene, M., Knox, J.E., Cross, J.B., Bakken, V., Adamo, C., Jaramillo, J., Gomperts, R., Stratmann, R.E., Yazyev, O., Austin, A.J., Cammi, R., Pomelli, C., Ochterski, J.W., Martin, R.L., Morokuma, K., Zakrzewski, V.G., Voth, G.A., Salvador, P., Dannenberg, J.J., Dapprich, S., Daniels, A.D., Farkas, Ö., Foresman, J.B., Ortiz, J.V., Cioslowski, J., Fox, D.J.: Gaussian 09, Revision D.01: Gaussian, Inc.: Wallingford CT (2009).
28. Dennington, R., Keith, T., Millam, J.: Gauss View, Version 5, Semichem Inc.: Shawnee Mission KS (2009).
29. Harata, K.: The structure of the cyclodextrin complex. XX. Crystal structure of uncomplexed hydrated γ-cyclodextrin. Bull. Chem. Soc. Jpn. **60**, 2763–2767 (1987)
30. Lipkowitz, K.B., Pearl, G., Coner, B., Peterson, M.A.: Explanation of where and how enantioselective binding takes place on permethylated β-cyclodextrin, a chiral stationary phase used in gas chromatography. J. Am. Chem. Soc. **119**, 600–610 (1997)
31. Badea, S.L., Vogt, C., Gehre, M., Fischer, A., Danet, A.F., Richnow, H.H.: Development of an enantiomer-specific stable carbon isotope analysis (ESIA) method for assessing the fate of α-hexachlorocyclohexane in the environment. Rapid Commun. Mass Spectrom. **25**, 1363–1372 (2011)
32. Kouno. H., Imasaka, T.: Efficiencies of resonant and nonresonant multiphoton ionization in the femtosecond region. Analyst DOI: 10.1039/c6an00577b
33. Castillejo, M., Couris, S., Koudoumas, E., Martín, M.: Subpicosecond ionization and dissociation of benzene and cyclic alkanes at 800 and 400 nm. Chem. Phys. Lett. **289**, 303–310 (1998)
34. Castillejo, M., Martín, M., Nalda, R.D., Couris, S., Koudoumas, E.: Dissociative ionization of halogenated ethylenes in intense femtosecond laser pulses. Chem. Phys. Lett. **353**, 295–303 (2002)
35. Kalcic, C.L., Gunaratne, T.C., Jones, A.D., Dantus, M., Reid, G.E.: Femtosecond laser-induced ionization/dissociation of protonated peptides. J. Am. Chem. Soc. **131**, 940–942 (2009)
36. Hamachi, A., Okuno, T., Imasaka, T., Kida, Y., Imasaka, T.: Resonant and nonresonant multiphoton ionization processes in the mass spectrometry of explosives. Anal. Chem. **87**, 3027–3031 (2015)